Promotion of Carbon-Supported Platinum−Ruthenium Catalyst for Electrodecomposition of Methanol

Kuan-Wen Wang,[†,‡] Sheng-Yang Huang,[†] and Chuin-Tih Yeh*[,‡]

Department of Chemistry, National Tsing Hua University, Hsinchu 300, Taiwan, and Fuel Cell Center, Yuan Ze University, Taoyuan 320, Taiwan

Received: December 8, 2006; In Final Form: January 23, 2007

A bimetallic catalyst consisting of a 7 wt % $Pt_{70}-Ru_{30}/C$ was prepared by the coprecipitation method and activated by a hydrogen reduction at 470 K. Physical characterization by TPR indicated that Pt atoms in the bimetallic crystallites deposited on freshly prepared catalysts tended to segregate to the crystallite surface during the activation. Catalytic activity of activated catalysts was examined by CV for oxidation of methanol. Current density obtained from the bimetallic catalyst was found to be enhanced by a combination of physical promotion with CeO_2 and chemical treatment of oxidation. The extent of enhancement varied with the loading of CeO_2 promoter and the temperature of oxidation treatment. A dramatic (370%) increase in the current density resulted from a promotion of 15% CeO_2 and an oxidation treatment at 570 K. Models for changes of the physical structure of deposited bimetallic crystallites on the CeO_2 promotion and the oxidation treatment are proposed on the basis of the results presented here.

1. Introduction

The direct methanol fuel cell (DMFC) is a promising candidate for a future energy source because of convenient fuel feeding and easy operation at low temperature.[1,2] However, the poor performance of the anode, the high cost of the membrane, methanol crossover from the anode to the cathode, and the expensive noble metal for the catalyst prevent the commercialization of DMFC.[2−4] On the anode front, there is an urgent need to enhance the catalytic performance as well as decrease the loading of noble metal.

Bimetallic Pt−Ru/C is widely regarded as the state-of-art catalyst to decompose methanol at the anode of the DMFC. Performance of the bimetallic catalyst can be enhanced by the addition of some promoters. These include metals,[5−7] oxides,[8−11] and nonmetals,[12] as well as appropriate heat treatments.[13,14] Substitution of catalyst support, from commercial carbon powders of XC-72 to carbon nanotubes, has also been suggested.[4,15]

Alloy particles on Pt−Ru/C catalysts are generally $d_{PtRu} \approx 3$ nm in size. Activity of the bimetallic catalysts depends heavily on the surface composition of their active ingredients. The surface composition of particles of this size cannot be easily characterized by conventional methods such as electron spectroscopy (XPS or Auger). On the basis of the ratio of coordination numbers with Pt and Ru, Liu et al.[16] and Hwang et al.[17] have developed an EXAFS (extended X-ray absorption fine structure) method to examine the surface enrichment of a metal component in bimetallic particles deposited on commercial PtRu/C catalysts.

In our laboratory, the temperature-programmed reduction (TPR) technique has been used to reduce oxygen chemisorbed on PtRu/C catalysts.[18] The adsorption may exhibit different stoichiometries as given below

$$2Pt + xO_2 \rightarrow PtO_{x,ad} \quad (1)$$

$$2Ru + yO_2 \rightarrow RuO_{y,ad} \quad (2)$$

The stoichiometries x and y in these two equations are found to vary with the size of the metal particles and the temperature of adsorption.

The temperature (T_r) required to reduce oxygen chemisorbed on Pt and Ru by TPR has been investigated in a previous report.[18] Oxygen chemisorbed on Ru exhibited a higher reduction temperature (T_r = 370 K) than that (T_r = 250 K) chemisorbed on Pt.

$$RuO_{ad} + H_2 \rightarrow Ru + H_2O \quad (3)$$

$$PtO_{ad} + H_2 \rightarrow Pt + H_2O \quad (4)$$

For oxygen adsorbed on PtRu alloy particles, T_r varies with their surface composition. A Pt-rich surface has a $T_r \approx 270$ K. A Ru-rich surface displays a higher T_r (∼320 K). Therefore, TPR could be an alternate technique to probe surface composition of PtRu alloy particles deposited on Pt−Ru/C catalysts.[18]

In this study, electroactivity of the PtRu/C catalyst for methanol oxidation was promoted by a combination of CeO_2 addition and oxidation treatments. Variation in surface and bulk composition of the deposited bimetallic crystallite on the promoted catalysts was characterized by using TPR and XRD.[18] The promotion effect can be satisfactorily explained by the variation in the surface composition and the structure of bimetallic crystallites.

2. Experimental Section

2.1. Preparation of Catalysts. Supported bimetallic catalysts of 7 wt % $Pt_{70}-Ru_{30}/Ce_xC$ (the weight ratio of Pt to Ru is 70:30) of varying cerium content (x, 0−20 wt % of cerium) were

* To whom correspondence should be addressed. E-mail: ctyeh@mx.nthu.edu.tw. Fax: 886-3-5711082. Tel: 886-3-5726047.
† National Tsing Hua University.
‡ Yuan Ze University.

10.1021/jp068456b CCC: $37.00
Published on Web 03/15/2007

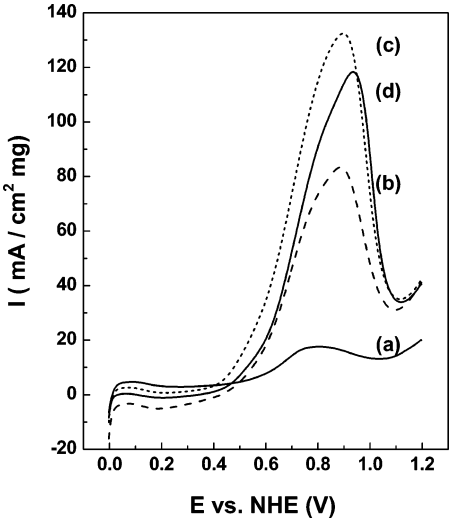

Figure 1. Forward scans of CV results for fresh (a) PtRu/C, (b) PtRu/$Ce_{10}C$, (c) PtRu/$Ce_{15}C$, and (d) PtRu/$Ce_{20}C$ samples.

prepared by the precipitation−deposition method. Metal ions of $PtCl_4$ (Merck), $RuCl_3$ (Strem), and $Ce(NO_3)_3$ (Fluka) in an aqueous solution were co-deposited at 340 K onto commercial carbon black (Vulcan XC-72) by 1 M NaOH at pH 8.0. The deposited catalysts were subsequently washed with DI water, dried at 320 K for 24 h, reduced in flowing H_2/N_2 (10/90 vol %) for 1 h at 470 K, and then stored as fresh catalysts.

Some of the fresh catalyst, PtRu/$Ce_{15}C$, is separated into different portions for 1 h oxidation treatment at predetermined temperatures (T_o, ranging from 420 to 620 K) under flowing air at a flow rate of 100 mL min^{-1}.

2.2. Characterization of Catalysts. Phase structures and compositions of fresh and oxidized catalysts were examined by X-ray diffraction (XRD, by Rigaku with Cu Kα radiation operated at 40 kV and 30 mA at a scan rate of 1°/min). Scherrer's equation was used to calculate the grain size of various samples. Surface composition of alloy catalysts was characterized by TPR. For the fresh samples, an oxygen adsorption step was followed at 300 K before the TPR measurements. Adsorbed samples were reduced by a flow of 10% H_2 in N_2 at a flow rate of 30 mL min^{-1} by raising the temperature from 80 to 450 K at a rate of 7 K min^{-1}. Temperature profiles and the rate of hydrogen consumption were measured by a thermal conductivity detector (TCD). TGA was performed, using a Seiko SSC 5000 thermal analyzer with a scan rate of 10 K min^{-1} under flowing air at a rate of 100 mL min^{-1} to obtain temperature profiles of weight loss caused by thermal desorption and carbon oxidation of prepared catalysts.

A CH Instruments model 600B cyclic voltammeter (CV) was used to characterize activity of prepared catalysts for methanol oxidation. Tested catalysts (including a commercial catalyst of 10 wt % $Pt_{70}-Ru_{30}$/C from E-TEK for comparison) of 20 mg were dispersed in 1 mL 2-propanol (Fluka) and then vibrated for 30 min in an ultrasonic bath to produce them into an ink. A sample of 4 mg ink was brushed onto a carbon paper (2 × 2 cm^2, ElectroChem EC-TP1-060) as catalyst on the working electrode. An electrochemical cell, consisting of a working electrode, a platinum film counter electrode, an Ag/AgCl reference electrode, and an electrolyte solution (consisting of 1.0 M CH_3OH and 0.5 M H_2SO_4) was used for all electrochemical measurements. Cyclic potentials were swept between 0.0 and 1.2 V (vs NHE) in a rate of 20 mV s^{-1} at room temperature. The electrolyte was prepurged with N_2 for 30 min before each CV experiment. All of the reported CV profiles were recorded at the sixteenth cycle.

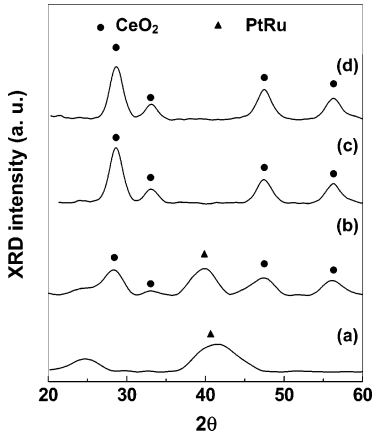

Figure 2. XRD patterns of fresh (a) PtRu/C, (b) PtRu/$Ce_{10}C$, (c) PtRu/$Ce_{15}C$, and (d) PtRu/$Ce_{20}C$ samples.

3. Results and Discussion

3.1. Promotion of CeO_2 to PtRu/Ce_xC Catalysts. Figure 1 gives a comparison of the forward scans of CV from methanol electro-oxidation over the alloy catalysts of PtRu/Ce_xC with different CeO_2 contents (x). The current density (I) of each scan increased initially with applied potential (E) after $E > \eta$ (onset potential, ~0.2 V), reached a maximum (I_{max}), and decreased on further increasing of E. The initial increase may be caused by methanol oxidation over Pt active sites following the reaction

$$CH_3OH + * \rightarrow 4H^+ + 4e^- + * - CO \qquad (5)$$

where $*$ represents a Pt site on the surface of bimetallic crystallites. The site is poisoned by the intermediate CO. Therefore, a depoison step is necessary for a regeneration of the active site which follows the reaction

$$*-CO + H_2O \rightarrow CO_2 + 2\,H^+ + * \qquad (6)$$

A catalyst with high activity for step 6 should give a high I_{max} current.[19] The rate of step 6 depends on the catalyst used. Accordingly, I_{max} depicted in Figure 1 may provide the information on the effectiveness of different PtRu/C catalysts to step 6. The same information may be found from the oxidation peak at the reverse scans (please refer to Figure S1

TABLE 1: CV, TPR, and XRD Characterizations of Fresh PtRu/Ce_xC Samples

			XRD	TPR[a]	
fresh catalysts	I_{max} (mA cm^{-2} mg^{-1})	I_{05} (mA cm^{-2} mg^{-1})	species	T_r/K	surface species
PtRu/C	17.6	4.7	PtRu	290, 310	AO_x
PtRu/$Ce_{10}C$	82.8	5.6	CeO_2, PtRu	280	AO_x
PtRu/$Ce_{15}C$	132.5	13.5	CeO_2	231, 248	Pt^sO_x
PtRu/$Ce_{20}C$	118.3	7.1	CeO_2	240, 265	$Pt^sO_x + AO_x$

[a] For TPR analysis, the samples were oxidized at 300 K.

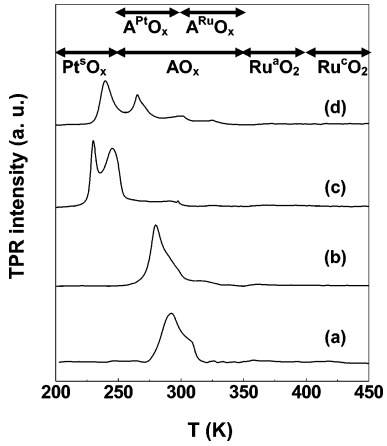

Figure 3. TPR analyses of fresh samples after oxidation at 300 K. (a) PtRu/C, (b) PtRu/Ce_{10}C, (c) PtRu/Ce_{15}C, and (d) PtRu/Ce_{20}C catalysts.

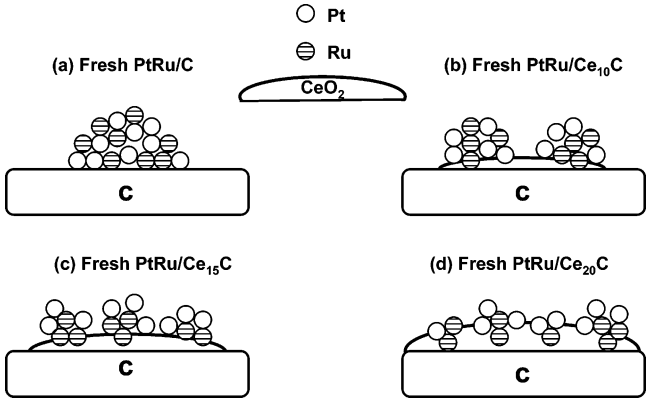

Figure 4. Schematic models of fresh PtRu/Ce_xC catalysts. (a) PtRu/C, (b) PtRu/Ce_{10}C, (c) PtRu/Ce_{15}C, and (d) PtRu/Ce_{20}C.

in the Supporting Information). On the other hand, the I_{05} value gives another hint about the numbers of active Pt sites working (N_{Pt}) under the practical condition of $E = 0.5$ V.

The second and the third columns of Table 1 compare the peak potential current (I_{max}) and current density at an applied potential of 0.5 V (I_{05}), respectively. Experimental I_{max} and I_{05} were found to increase with the amount of CeO_2 added in low values of x, reached a maximum at $x = 15\%$, and decreased upon increasing x further. A 3-fold increase of I_{05} was found from the sample with optimized CeO_2 promotion (15%), compared to the unpromoted PtRu/C catalyst.

The promotion of CeO_2 can be explained in detail by XRD characterization. Figure 2 gives a comparison of the XRD patterns of the fresh PtRu/Ce_xC catalysts. Besides a diffraction at $2\theta = 25°$ from graphite, the Figure 2a showed a very broad peak at $2\theta = 40°$ for the (111) diffraction of PtRu fcc alloy in the unpromoted PtRu/C. The broadness of this peak indicates that alloy particles deposited have an average size of $d_{alloy} = 2$ nm. The intensity of PtRu peaks decreased on increasing the CeO_2 promotion and became unnoticeable on increasing $x >$ 15% (Figure 2c,d). Conceivably, the sizes of bimetallic particles deposited on PtRu/Ce_xC catalysts decreased upon increasing the CeO_2 promotion. Therefore, the CeO_2 added in PtRu/Ce_xC may be regarded as a textural promoter (a promoter that affects the physical size of active components in catalysts) that increases the dispersion of supported bimetallic catalysts.

A set of additional peaks corresponding to CeO_2 diffraction were found in XRD patterns in Figure 2 for PtRu/C catalysts with CeO_2 promotion. The intensity of the peak generally increases with x. The broadness of these peaks indicated that

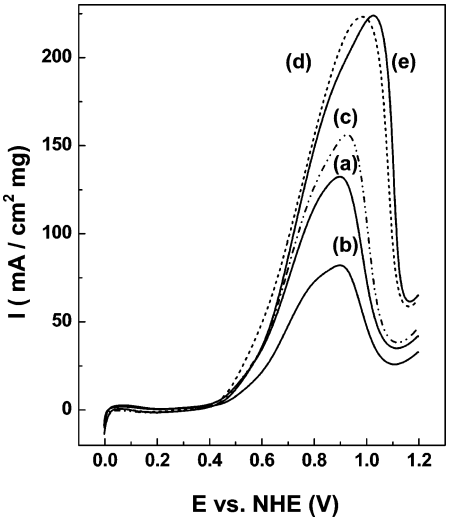

Figure 5. Forward scans of CV results for (a) fresh PtRu/Ce_{15}C sample after oxidation at (b) 420 K, (c) 520 K, (d) 570 K, and (e) 620 K. The weight loss caused by oxidation treatment was also considered.

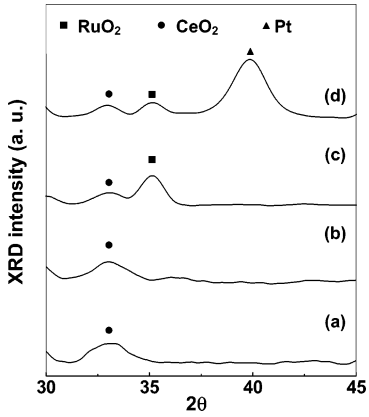

Figure 6. XRD patterns of PtRu/Ce_{15}C samples after oxidation at (a) 420 K, (b) 520 K, (c) 570 K, and (d) 620 K.

the average size of CeO_2 deposited increased slightly (from 3 to 5 nm) when the CeO_2 promotion is increased.

The TPR technique is a surface-sensitive detector to probe surface composition of bimetallic particles deposited on PtRu/C catalysts.[18] Figure 3 compares a series of TPR traces from the fresh PtRu/Ce_xC preadsorbed with oxygen for 1 h at room temperature. These oxidized catalysts showed various reductive peaks at different T_r. According to assignments of a previous study (shown in the top of Figure 3), peaks with T_r located between 230 and 250 K, between 250 and 350 K, and above 350 K may be attributed to reduction of Pt^sO_x, AO_x, and RuO_2, respectively.[18]

On the basis of the T_r position of different TPR traces in Figure 3, composition of the surface of bimetallic crystallites dispersed on PtRu/Ce_xC catalysts are listed in the last column of Table 1. Bimetallic crystallites deposited on the nonpromoted PtRu/C catalyst were coated with a surface layer of oxidized Pt−Ru alloy (AO_x, $T_r = 300$ K at trace 3a). The fraction of Pt (F_{Pt}) on surface of bimetallic crystallites was increased upon a light promotion of PtRu/C with Ce ($x < 15$). As a result, T_r positions of traces 3b and 3c gradually decreased to 250 K. However, the surface of heavily promoted PtRu/Ce_{20}C was mildly contaminated with Ru (trace 3d).

Precipitation−deposition is a common method found in literature for preparation of PtRu/C bimetallic catalysts. PtRu alloy particles deposited on these catalysts prepared by this

TABLE 2: CV, TPR, and XRD Characterizations of the Various as-Oxidized PtRu/Ce_{15}C Samples

			XRD	TPR	
catalyst (PtRu/Ce_{15}C)	I_{max} (mA cm^{-2} mg^{-1})	I_{05} (mA cm^{-2} mg^{-1})	species	T_r/K	oxidized species
O300	132.5	13.5	CeO_2	231, 248	Pt^sO_x
O420	82.1	7.8	CeO_2	280, 322	AO_x
O520	156.3	13.3	CeO_2, RuO_2(w)[a]	295, 320	AO_x
O570	223.4	17.6	CeO_2, RuO_2(s)[b]	302	AO_x
O620	225.0	12.6	CeO_2, Pt, RuO_2(s)[b]	280, 420	$AO_x + Ru^cO_2$

[a] w: weak peak. [b] s: strong peak.

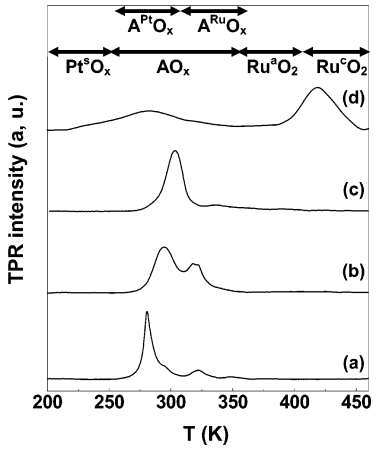

Figure 7. TPR analyses of PtRu/Ce_{15}C samples after oxidation at (a) 420 K, (b) 520 K, (c) 570 K, and (d) 620 K.

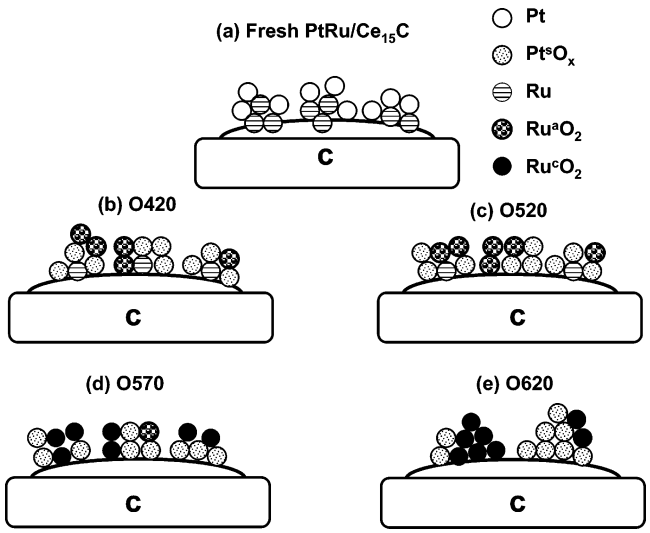

Figure 8. Schematic models for (a) fresh PtRu/Ce_{15}C sample after oxidation at (b) 420 K, (c) 520 K, (d) 570 K, and (e) 620 K.

method generally have a Pt inner core and Ru outer shell structure.[18,20] Upon activation of the PtRu/C hydrogen reduction, Pt atoms in the core in the deposited crystallites had a tendency to segregate to their surface.[18] Accordingly, F_{Pt} of bimetallic crystallites on prepared catalyst may be increased by segregation during reduction treatment. The segregation would be prominent for small-sized bimetallic crystallites.

Figure 4 gives a schematic variation of bimetallic crystallites on fresh PtRu/Ce_xC catalysts with different promotion of CeO_2. According to XRD characterization, the sizes of bimetallic particles generally decreased as a result of the CeO_2 promotion. F_{Pt} on the surface of the reduced particles can be interpreted by the extent of Pt segregation during the reduction activation. F_{Pt} of the resultant bimetallic crystallites increased as Ce content in Pt−Ru/Ce_xC increased. The surface of bimetallic crystallites dispersed on Pt−Ru/Ce_{15}C was almost completely covered by Pt ($F_{Pt} \rightarrow 100\%$) as the CeO_2 content was increased to 15%. Since Pt is the active site of methanol decomposition, I_{05} was found in the second column of Table 1 to increase from 4.7 to 13.5 mA cm^2 mg^{-1} upon addition of 15% CeO_2 to the Pt−Ru/C. The I_{05} increase may be attributed to a simultaneous increase of F_{Pt} (demonstrated in Figure 4c) and decrease in the size (d_{Pt-Ru}) of bimetallic crystallites. However, I_{05} of PtRu/Ce_xC is found to decrease slightly upon further increase of the CeO_2 contents to $x = 20$. Reduction in activity may be attributed to a partial occlusion of bimetallic crystallites in CeO_2.[9] Occluded crystallites may be inactive for the methanol oxidation.

Interestingly, the F_{Pt} of bimetallic crystallites deposited on PtRu/Ce_xC decreased upon increasing the Ce promotion from $x = 15$ to 20. TPR trace 3d suggested that oxygen adsorbed on PtRu/Ce_{20}C catalysts generated not only Pt^sO_x but also AO_x. It is likely that the surface of activated bimetallic crystallites might have been covered by a small fraction of Ru (with $F_{Pt} < 100\%$). The binary Pt−Ru surface might have been caused by an increase in metallic dispersion ($D > 50\%$). As a result, platinum atoms in the crystallites are not abundant enough to cover their surface.[9]

3.2. Enhancement of the Activity Of PtRu/Ce_{15}C Catalysts by Oxidation. Figure 1 indicates that PtRu/Ce_{15}C is the most active catalyst prepared in this study for electrodecomposition of methanol. We are interested in finding whether the activity of this catalyst can be further increased by oxidation treatment. Figure 5 shows the forward scans of CV from PtRu/Ce_{15}C samples preoxidized at different T_o.

Columns 2 and 3 of Table 2 compare the variation of I_{max} and I_{05} of PtRu/C_{15}C catalysts oxidized at different T_o. Both I_{max} and I_{05} are found to decrease upon oxidation at low T_o (420 K) and increase upon raising T_o of the oxidation treatment. An optimized oxidation treatment was found at $T_o = 570$ K when the highest specific current densities of $I_{max} = 223.4$ and $I_{05} = 17.6$ mA cm^{-2} were attained. Noticeably, the I_{05} of this sample is around 3 times higher than that measured from a commercial E-TEK $(PtRu)_{10}$/C catalyst (please refer to Supporting Information Figure S3).

Figure 6 gives a comparison of the XRD patterns from PtRu/Ce_{15}C catalysts oxidized at different temperatures (T_o =420−620 K). Similar to the pattern of fresh PtRu/Ce_{15}C (Figure 2c), negligible diffraction from bimetallic crystallites was found from catalysts oxidized at low T_o (Figure 6a,b). However, a peak of crystalline RuO_2 (Ru^cO_2, $2\theta = 35°$) was observed from catalysts oxidized at $T_o > 570$ K (Figure 6c,d), and an additional peak for sintered Pt ($d_{Pt} \approx 4.5$ nm) was also observed from the catalyst oxidized at $T_o = 620$ K. Column 4 of Table 2 lists species detected from the catalyst PtRu/C_{15}C oxidized at different T_o.

TPR also provides variation of the surface composition of bimetallic crystallites on PtRu/C catalysts upon increasing T_o. Trace c of Figure 3 suggested that bimetallic crystallites on

freshly reduced PtRu/C catalyst had a structure with Ru inner core and Pt outer surface. The TPR traces shown in Figure 7 give more information about the effect of oxidation treatment. Peaks in traces 7a−7c have a reduction temperature of $T_r >$ 270 K, with area generally increased as T_o, the temperature of the oxidation treatment, is increased. As seen from the calibration at the top of this figure, the surfaces of bimetallic crystallites on oxidized catalysts were covered by oxides of alloys. The fraction of Ru (F_{Ru}) segregated to the surface also increased with T_o. Oxidized Ru had a high tendency to aggregate. The tendency was caused probably by of phase separation of Ru^cO_2 from bimetallic crystallites upon oxidation at $T_o = 620$ K.

Figure 8 provides a model which describes the structure change, as characterized by XRD and TPR, of bimetallic crystallites deposited on $PtRu/Ce_{15}C$ catalysts during oxidation treatments with increasing T_o. The surface of crystallites on freshly reduced catalyst had a Pt-rich outer surface and Ru-rich inner core structure (Figure 8a). Pt was oxidized to Pt^sO_x, and Ru was oxidized to amorphous RuO_2 (Ru^aO_2) upon mild oxidation at $T_o = 420$ K. Since Ru has a higher affinity to oxygen than Pt, Ru^aO_2 tends to segregate to the surface of crystallites (Figure 8b) at elevated temperatures. The segregation became extensive (Figure 8c) and the accumulated Ru^aO_2 gradually coagulated (Figure 8d) to Ru^cO_2 on increasing the T_o above 520 K. Upon oxidation at high temperature of $T_o = 620$ K, a sintering of dispersed particles as well as a phase separation of Ru^cO_2 occurred concomitantly.

Figure 5 indicates that current density of methanol oxidation over $Pt-Ru/Ce_{15}C$ catalyst is noticeably affected by oxidation treatment. The variation in current density upon increasing the T_o of oxidation treatment may be explained in terms of two factors: a decrease in the rate of reaction 5 due to chemical segregation of Ru to the surface (i.e., F_{Pt} was decreased) and a promotion of reaction 6 by formation of Ru^cO_2. These two factors affected the current density in opposite directions. The segregation caused a decrease in current density at oxidation at $T_o = 420$ K. However, the segregation effect was surpassed by the formation of Ru^cO_2 at high $T_o > 520$ K. Promoter Ru^cO_2 is found to be more active and stable than Ru or Ru^aO_2. This result is consistent with Rolison's observation that the bimetallic alloy is not the most desired form of catalyst, and RuO_xH_y (hydrated RuO_2) is a much more active catalyst for methanol oxidation than Ru.[21,22]

4. Conclusions

In this study, an enhancement of the electroactivity of PtRu/C catalyst on methanol decomposition by a combination of CeO_2 promotion and oxidation treatment has been tried. The following information was obtained.

1. A 370% enhancement in the electroactivity may be obtained by an optimized promotion, with a loading of $CeO_2 \approx 15\%$, and oxidation at $T_o = 570$ K.

2. The CeO_2 promotion may be attributed to an increase in the dispersion of PtRu crystallites and/or an enrichment of Pt to the surface of bimetallic crystallites.

3. The oxidation promoted the formation of a stable Ru^cO_2 phase in the bimetallic crystallites. The enhancement is optimized at $T_o = 570$ K.

4. The TPR technique can be used as an excellent tool to analyze the top surface composition of bimetallic crystallites.

Acknowledgment. The authors appreciate the National Science Council and the Educational Ministry of the Republic of China for financial support on this study.

Supporting Information Available: Additional CV data as mentioned in the text. This material is available free of charge via the Internet at http://pubs.acs.org.

References and Notes

(1) Hamnett, A. *Catal. Today* **1997**, *38*, 445.
(2) Ren, X.; Wilson, M. S.; Gottesfeld, S. *J. Electrochem. Soc.* **1996**, *143*, L12.
(3) Hogarth, M. P.; Ralph, T. R. *Platinum Metals Rev.* **2002**, *46*, 146.
(4) Prabhuram, J.; Zhao, T. S.; Tang, Z. K.; Chen, R.; Liang, Z. X. *J. Phys. Chem. B* **2006**, *110*, 5245.
(5) Liang, Y.; Zhang, H.; Zhong, H.; Zhu, X.; Tian, Z.; Xu, D.; Yi, B. *J. Catal.* **2006**, *238*, 468
(6) Liang, Y.; Zhang, H.; Tian, Z.; Zhu, X.; Wang, X.; Yi, B. *J. Phys. Chem. B* **2006**, *110*, 7828.
(7) Park, K. W.; Choi, J. H.; Lee, S. A.; Pak, C.; Chang, H.; Sung, Y. E. *J. Catal.* **2004**, *224*, 236.
(8) Park, K. W.; Sung, Y. E.; Toney, M. F. *Electrochem. Commun.* **2006**, *8*, 359.
(9) Huang, S. Y.; Chang, C. M.; Yeh, C. T. *J. Catal.* **2006**, *241*, 400.
(10) Guo, J. W.; Zhao, T. S.; Prabhuram, J.; Chen, R.; Wong, C. W. *J. Power Sources* **2006**, *156*, 345.
(11) Xu, C.; Shen, P. K. *J. Power Sources* **2005**, *142*, 27.
(12) Daimon, H.; Kurobe, Y. *Catal. Today* **2006**, *111*, 182.
(13) Lu, Q.; Yang, B.; Zhuang, L.; Lu, J. *J. Phys. Chem. B* **2005**, *109*, 8873.
(14) Li, X.; Hsing, I. M. *Electrochim. Acta* **2006**, *52*, 1358.
(15) Liao, S.; Holmes, K. A.; Tsaprailis, H.; Birss, V. I. *J. Am. Chem. Soc.* **2006**, *128*, 3504.
(16) Liu, D. G.; Lee, J. F.; Tang, M. T. *J. Mol. Catal. A: Chem.* **2005**, *240*, 197.
(17) Hwang, B. J.; Sarma, L. S.; Chen, J. M.; Chen, C. H.; Shih, S. C.; Wang, G. R.; Liu, D. G.; Lee, J. F.; Tang, M. T. *J. Am. Chem. Soc.* **2005**, *127*, 11140.
(18) Huang, S. Y.; Chang, C. M.; Yeh, C. T. *J. Phys. Chem. B* **2006**, *110*, 234.
(19) Manoharan, R.; Goodenough, J. B. *J. Mater. Chem.* **1992**, *2*, 875.
(20) Hwang, B. J.; Chen, C. H.; Sarma, L. S.; Chen, J. M.; Wang, G. R.; Tang, M. T.; Liu, D. G.; Lee, J. F. *J. Phys. Chem. B* **2006**, *110*, 6475.
(21) Long, J. W.; Stroud, R. M.; Swider-Lyons, K. E.; Rolison, D. R. *J. Phys. Chem. B* **2000**, *104*, 9772.
(22) Rolison, D. R.; Hagans, P. L.; Swider, K. E.; Long, J. W. *Langmuir* **1999**, *15*, 774.